Canadian Geotechnical Journal
Published by
THE NATIONAL RESEARCH COUNCIL OF CANADA

Revue canadienne de géotechnique
Publié par
LE CONSEIL NATIONAL DE RECHERCHES DU CANADA

Volume 15 Number 3 August 1978 Volume 15 numéro 3 août 1978

The shear strength of unsaturated soils

D. G. FREDLUND
University of Saskatchewan, Saskatoon, Sask., Canada S7N 0W0
AND
N. R. MORGENSTERN
University of Alberta, Edmonton, Alta., Canada T6G 2G7
AND
R. A. WIDGER
Department of Highways, Prince Albert, Sask., Canada S6V 5S4

Received June 1, 1977
Accepted February 1, 1978

The shear strength of an unsaturated soil is written in terms of two independent stress state variables. One form of the shear strength equation is

$$\tau = c' + (\sigma - u_w) \tan \phi' + (u_a - u_w) \tan \phi''$$

The transition from a saturated soil to an unsaturated soil is readily visible. A second form of the shear strength equation is

$$\tau = c' + (\sigma - u_a) \tan \phi' + (u_a - u_w) \tan \phi^b$$

Here the independent roles of changes in total stress σ and changes in pore-water pressure u_w are easily visualized.

Published research literature provides limited data. However, the data substantiate that the shear strength can be described by a planar surface of the forms proposed. A procedure is also outlined to evaluate the pertinent shear strength parameters from laboratory test results.

La résistance au cisaillement d'un sol non saturé est écrite en fonction de deux variables d'état de contrainte indépendantes. Une forme de l'équation de résistance au cisaillement est

$$\tau = c' + (\sigma - u_w) \tan \phi' + (u_a - u_w) \tan \phi''$$

Le passage de l'état saturé à l'état non saturé est évident. Une deuxième forme de cette équation est

$$\tau = c' + (\sigma - u_a) \tan \phi' + (u_a - u_w) \tan \phi^b$$

Dans ce cas, les influences réciproques des changements dans la contrainte totale σ et des changements dans la pression interstitielle u_w sont facilement observables.

Peu de données sont disponibles dans la littérature. Cependant, ces données établissent que la résistance au cisaillement peut être décrite par une surface plane ayant les formes proposées. Une procédure est également décrite pour évaluer les paramètres pertinents de la résistance au cisaillement en partant de résultats d'essais de laboratoire.

[Traduit par la revue]

Introduction

During the past two decades there has been an increasing use of two independent stress variables to describe the behavior of unsaturated soils (Coleman 1962; Bishop and Blight 1963; Burland 1965; Aitchison 1967; Matyas and Radhakrishna 1968; Barden *et al.* 1969; Brackley 1971; Fredlund 1974; Fredlund and Morgenstern 1976, 1977). Most consideration has been given to describing the volume change behavior (and suitable constitutive relations) for unsaturated soils. Several investigations have been made into the shear strength characterization of unsaturated soils (Bishop *et al.* 1960; Massachusetts Institute of Technology (MIT) 1963; Sridharan 1968; Maranha das Neves 1971); however, none has proven completely successful.

Fredlund and Morgenstern (1977) showed from a stress field analysis that any two of three possible stress variables can be used to define the stress state in an unsaturated soil. Possible combinations are: (1) $(\sigma - u_a)$ and $(u_a - u_w)$, (2) $(\sigma - u_w)$ and $(u_a - u_w)$, and (3) $(\sigma - u_a)$ and $(\sigma - u_w)$, where σ = total normal stress, u_a = pore air pressure, and u_w = pore-water pressure. Null experiments (i.e. $\Delta\sigma = \Delta u_a = \Delta u_w$) supported the proposed theoretical stress state variables.

The objective of this paper is to present the shear strength of an unsaturated soil in terms of two independent stress state variables. The shear strength, using two possible combinations of stress state variables, is presented and the relationship between the two cases is shown. The first stress state variables used are $(\sigma - u_w)$ and $(u_a - u_w)$. The advantage of this combination of variables is that it provides a readily visualized transition from the unsaturated to the saturated case. The disadvantage arises in that, when the pore-water pressure is changed, two stress state variables are being affected. The relative significance of each variable must be borne in mind when considering the shear strength. (This is also the disadvantage associated with utilizing the $(\sigma - u_a)$ and $(\sigma - u_w)$ combination of stress state variables.)

The second combination of stress state variables used is $(\sigma - u_a)$ and $(u_a - u_w)$. The advantage of this combination is that only one stress variable is affected when the pore-water pressure is changed. Regardless of the combination of stress variables used to define the shear strength, the value of shear strength obtained for a particular soil with certain values of σ, u_a, and u_w must be the same.

Research data from the testing program of other workers are used to demonstrate the use of the proposed shear strength equations for unsaturated soils.

Theory

For a saturated soil, a stress circle corresponding to failure conditions is plotted on a two-dimensional plot of effective normal stress versus shear strength. A series of tests gives a line of failure (i.e. a Mohr–Coulomb failure envelope).

In the case of an unsaturated soil, the stress circle corresponding to the failure conditions must be plotted on a three-dimensional diagram. The axes in the horizontal plane are the stress state variables and the ordinate is the shear strength. A series of tests gives a surface defining failure conditions.

(a) Shear Strength in Terms of the $(\sigma - u_w)$ and $(u_a - u_w)$ Stress State Variables

The vertical plane of $(\sigma - u_w)$ versus shear strength, with $(u_a - u_w)$ equal to zero, corresponds to the case where the soil is saturated. If the soil has a positive matrix suction, i.e. $(u_a - u_w)$ is greater than zero, a third dimension is required to plot the stress circle. It is initially assumed that the surface defined by a series of tests, on unsaturated soil samples, is planar. Therefore, the equation defining the surface of failure can be written as an extension of the conventional saturated soil case:

$$[1] \quad \tau = c' + (\sigma - u_w) \tan \phi' + (u_a - u_w) \tan \phi''$$

where c' = effective cohesion parameter, ϕ' = the friction angle with respect to changes in $(\sigma - u_w)$ when $(u_a - u_w)$ is held constant, and ϕ'' = friction angle with respect to changes in $(u_a - u_w)$ when $(\sigma - u_w)$ is held constant. A three-dimensional plot of the stress state variables versus shear strength is difficult to analyze. Therefore, a procedure is outlined to assist in obtaining the desired shear strength parameters. For convenience in handling the strength data from triaxial tests, the stress point at the top of each stress circle can be used, i.e. $[\frac{1}{2}(\sigma_1 + \sigma_3) - u_w]$ and $(u_a - u_w)$. The equation for the plane through the stress points is

$$[2] \quad \tfrac{1}{2}(\sigma_1 - \sigma_3) = d' + [\tfrac{1}{2}(\sigma_1 + \sigma_3) - u_w] \tan \psi' + (u_a - u_w) \tan \psi''$$

where d' = the intercept when the two stress points are zero, ψ' = the angle between the stress point plane and the $[\frac{1}{2}(\sigma_1 + \sigma_3) - u_w]$ axis when $(u_a - u_w)$ is held constant, ψ'' = the angle between the stress point plane and the $(u_a - u_w)$ axis when

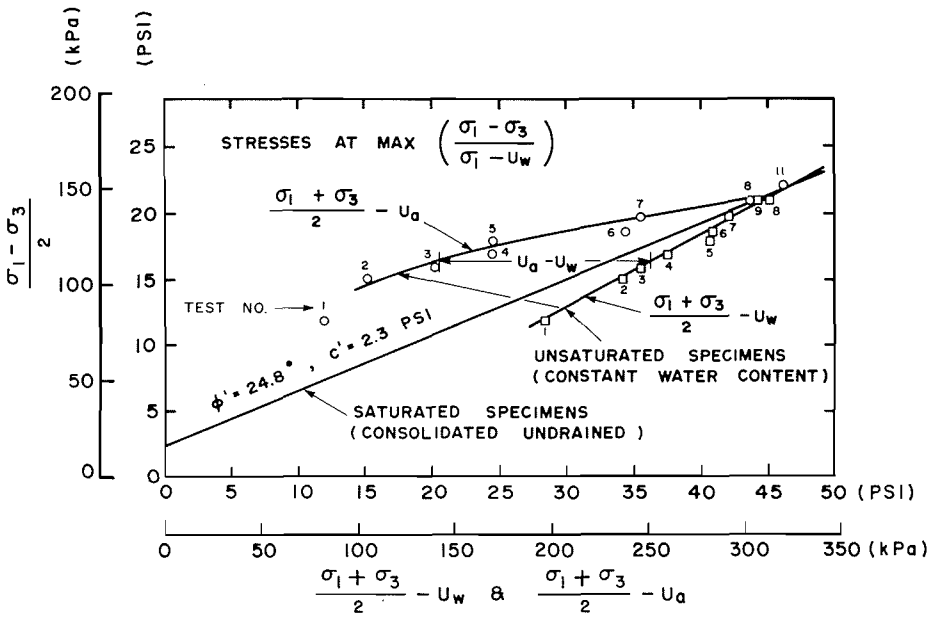

FIG. 1. Triaxial tests on a compacted shale (clay fraction 22%) compacted at a water content of 18.6% and sheared at constant water content (from Bishop *et al.* 1960).

$[\frac{1}{2}(\sigma_1 + \sigma_3) - u_w]$ is held constant. The relationship between a plane through the stress points and the failure surface is shown in the Appendix along with the corresponding soil parameters. It is necessary to plot the data in a special manner in order to obtain the ϕ'' friction parameters.

(b) Shear Strength in Terms of the $(\sigma - u_a)$ and $(u_a - u_w)$ Stress State Variables

The equation for the failure surface when $(\sigma - u_a)$ and $(u_a - u_w)$ are used as stress variables is

$$[3] \quad \tau = c'' + (\sigma - u_a) \tan \phi^a + (u_a - u_w) \tan \phi^b$$

where c'' = cohesion intercept when the two stress variables are zero; ϕ^a = the friction angle with respect to changes in $(\sigma - u_a)$ when $(u_a - u_w)$ is held constant; ϕ^b = friction angle with respect to changes in $(u_a - u_w)$ when $(\sigma - u_a)$ is held constant. The number of parameters, however, can be reduced. When the matrix suction is zero, the $(\sigma - u_a)$ plane will have the same friction angle parameter as the $(\sigma - u_w)$ plane when using the previous combination, (a), of stress state variables. Therefore, ϕ^a is the same as ϕ'. Also, c'' is the same as c'. The shear strength equation is now

$$[4] \quad \tau = c' + (\sigma - u_a) \tan \phi' + (u_a - u_w) \tan \phi^b$$

Equation 1 or 4 will give the same value for shear strength. Therefore, it is possible to equate them and obtain the relationship between the various angles of friction.

$$[5] \quad \tan \phi' = \tan \phi^b - \tan \phi''$$

Test Data

Published research literature reveals that few tests have been performed where the principal stresses and the pore-air and pore-water pressures have been measured as the specimen is loaded. Three sets of data are presented below.

(a) Compacted Shale (Bishop et al. 1960)

Triaxial tests were performed on a shale compacted at a water content of 18.6%. The clay content was 22%. All specimens were sheared at a constant water content. The failure envelope for tests on saturated specimens gave $\phi' = 24.8°$ and $c' = 15.8$ kPa (2.3 psi) (Fig. 1). The data for tests on unsaturated test specimens are plotted on Fig. 1 and summarized in Table 1. Figure 2 shows a plot of $[\frac{1}{2}(\sigma_1 + \sigma_3) - u_w]$ and $(u_a - u_w)$ versus $\frac{1}{2}(\sigma_1 - \sigma_3)$. It is obvious that this type of plot is not very useful since it is impossible to visualize the plane on which the points fall. As proposed in the Appendix, $(\Delta\tau_d \cos \psi')$ is plotted versus $(u_a - u_w)$ in order to obtain α (Fig. 3). The graphically obtained angle for the compacted shale is $\alpha = -3.9°$. This corresponds to a ψ'' value of $-4.2°$ and a ϕ'' value of $-4.6°$. One form of the shear strength equation would be

TABLE 1. Results for compacted shale (from Bishop *et al.* 1960)

Test No.	$\frac{1}{2}(\sigma_1 + \sigma_3) - u_a$ (kPa)	$\frac{1}{2}(\sigma_1 + \sigma_3) - u_a$ (psi)	$\frac{1}{2}(\sigma_1 + \sigma_3) - u_w$ (kPa)	$\frac{1}{2}(\sigma_1 + \sigma_3) - u_w$ (psi)	$\frac{1}{2}(\sigma_1 - \sigma_3)$ (kPa)	$\frac{1}{2}(\sigma_1 - \sigma_3)$ (psi)	$(u_a - u_w)$ (kPa)	$(u_a - u_w)$ (psi)	Calculated* $\frac{1}{2}(\sigma_1 - \sigma_3)$ (kPa)	Calculated* $\frac{1}{2}(\sigma_1 - \sigma_3)$ (psi)	$\Delta\tau_d$ (kPa)	$\Delta\tau_d$ (psi)	$\Delta\tau_d \cos\psi'$ (kPa)	$\Delta\tau_d \cos\psi'$ (psi)
1	81	11.8	196	28.4	82	11.9	114	16.6	97	14.0	−14	−2.1	−13	−1.9
2	104	15.1	236	34.2	103	15.0	132	19.1	113	16.4	−9.7	−1.4	−9.0	−1.3
3	139	20.1	243	35.3	110	16.0	105	15.2	117	16.9	−6.2	−0.9	−5.5	−0.8
4	168	24.4	258	37.4	117	17.0	90	13.0	123	17.8	−5.5	−0.8	−4.8	−0.7
5	168	24.4	280	40.6	123	17.9	112	16.2	132	19.1	−8.3	−1.2	−7.6	−1.1
6	236	34.2	281	40.7	128	18.6	45	6.5	132	19.2	−4.1	−0.6	−3.4	−0.5
7	243	35.3	289	41.9	137	19.8	46	6.6	136	19.7	0.7	0.1	0.7	0.1
8	301	43.6	310	45.0	147	21.3	9.7	1.4	145	21.0	2.1	0.3	2.1	0.3
9	302	43.8	302	43.8	145	21.1	0.0	0.0	141	20.4	4.8	0.7	4.1	0.6
10	305	44.3	305	44.3	145	21.1	0.0	0.0	143	20.7	2.8	0.4	2.1	0.3
11	316	45.9	316	45.9	153	22.2	0.0	0.0	148	21.4	5.5	0.8	5.5	0.8

*The calculated value refers to the shear stress on the saturation failure envelope.

[6] $\tau = 2.3 + (\sigma - u_w) \tan 24.8° - (u_a - u_w) \tan 4.6°$

The ϕ'' angle is negative since the pore-water pressure variable appears in both stress variables. The physical significance can be stated as follows:

A decrease in pore-water pressure u_w is not as efficient in increasing the $(\sigma - u_w) \tan \phi'$ component of strength as is a corresponding increase in total stress σ. Rather, decreasing the pore-water pressure increases the frictional resistance of the soil by (tan 24.8° − tan 4.6°), which is equal to tan 20.9°. On the basis of [5] the 20.9° angle is equal to ϕ^b. Therefore, another form of the shear strength equation is

[7] $\tau = 2.3 + (\sigma - u_a) \tan 24.8° + (u_a - u_w) \tan 20.9°$

From this equation, the relative shear strength contributions of the total stress and the pore-water pressures are readily inspected.

(b) Boulder Clay (Bishop et al. 1960)

These triaxial tests were performed on specimens compacted at a water content of 11.6% and sheared at a constant water content. The clay frac-

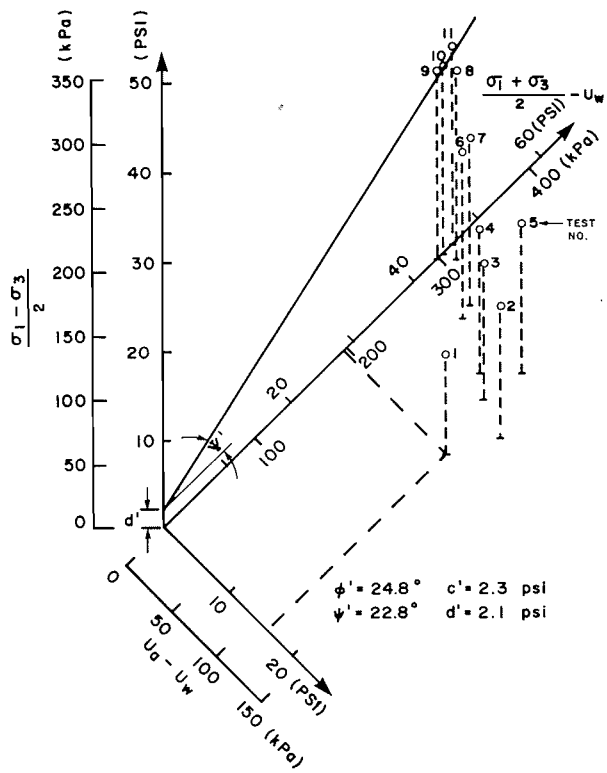

FIG. 2. Three-dimensional strength envelope for compacted shale.

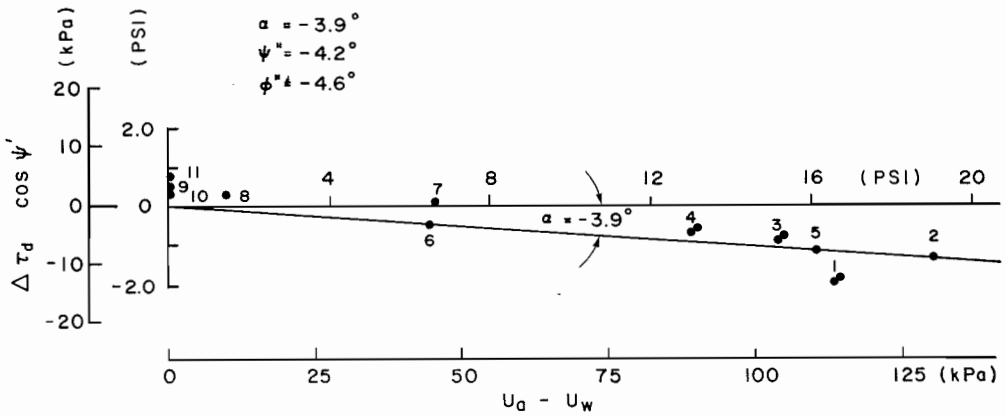

FIG. 3. Change in shear strength from saturated strength plane for compacted shale.

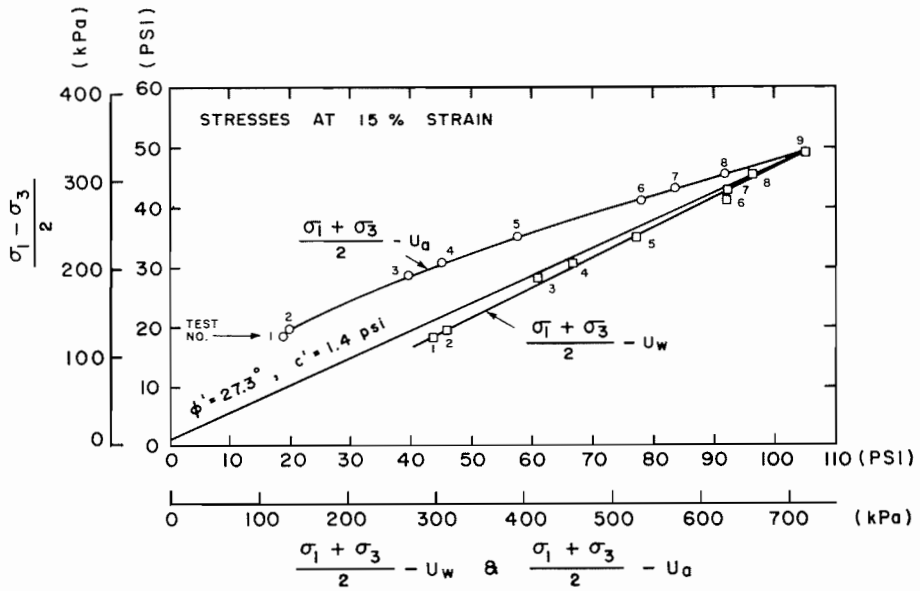

FIG. 4. Triaxial tests on a compacted Boulder clay (clay fraction 18%) compacted at a water content of 11.6% and sheared at constant water content (from Bishop *et al.* 1960).

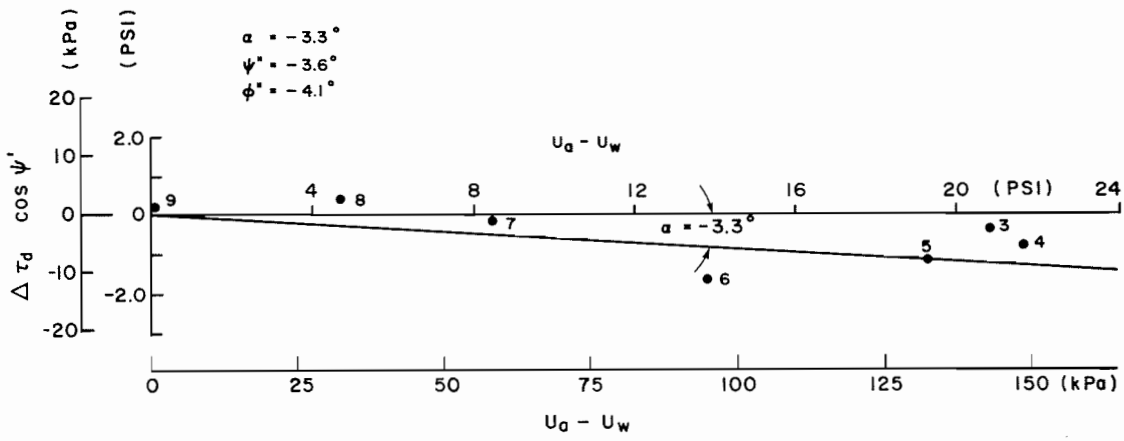

FIG. 5. Change in shear strength from saturated strength plane for Boulder clay.

TABLE 2. Results for compacted Boulder clay (from Bishop *et al.* 1960)

Test No.	$\frac{1}{2}(\sigma_1 + \sigma_3) - u_a$		$\frac{1}{2}(\sigma_1 + \sigma_3) - u_w$		$\frac{1}{2}(\sigma_1 - \sigma_3)$		$u_a - u_w$		Calculated* $\frac{1}{2}(\sigma_1 - \sigma_3)$		$\Delta\tau_d$		$\Delta\tau_d \cos\psi'$	
	(kPa)	(psi)	(kPa)	(psi)	(kPa)	(psi)	(kPa)	(psi)	(kPa)	(psi)	(kPa)	(psi)	(kPa)	(psi)
1	129	18.7	300	43.5	126	18.3	171	24.8	146	21.2	−14	−2.9	−18	−2.6
2	137	19.8	316	45.8	134	19.5	179	26.0	154	22.3	−14	−2.8	−17	−2.5
3	274	39.7	417	60.5	197	28.6	143	20.8	200	29.0	−2.8	−0.4	−2.1	−0.3
4	310	45.0	460	66.7	214	31.0	150	21.7	219	31.8	−5.5	−0.8	−4.8	−0.7
5	396	57.5	530	76.8	243	35.2	133	19.3	252	36.5	−9.0	−1.3	−7.6	−1.1
6	536	77.8	632	91.7	286	41.5	96	13.9	299	43.3	−12	−1.8	−11	−1.6
7	574	83.3	633	91.8	291	42.2	59	8.5	292	42.4	−1.4	−0.2	−1.4	−0.2
8	629	91.3	662	96.0	316	45.8	32	4.7	315	45.7	0.7	0.1	0.7	0.1
9	722	104.7	722	104.7	341	49.5	0.0	0.0	340	49.3	1.4	0.2	1.4	0.2

*The calculated value refers to the shear stress on the saturation failure envelope.

tion was 18%. The data are shown in Fig. 4 and summarized in Table 2. The saturated specimens gave a ϕ' angle equal to 27.3° and an effective cohesion $c' = 9.6$ kPa (1.4 psi). Figure 5 shows the $(\Delta\tau_d \cos\psi')$ versus $(u_a - u_w)$ plot. The best fit line gives an angle $\alpha = -3.3°$. The corresponding angles $\psi'' = -3.6°$ and $\phi'' = -4.1°$. The ϕ^b angle is 24.0°. The forms of the shear strength equation for the Boulder clay are:

$$[8] \quad \tau = 1.4 + (\sigma - u_w) \tan 27.3° - (u_a - u_w) \tan 4.1°$$

$$[9] \quad \tau = 1.4 + (\sigma - u_a) \tan 27.3° + (u_a - u_w) \tan 24.0°$$

The interpretation of [8] and [9] is the same as for equations [6] and [7].

(c) Potters Flint and Peerless Clay (MIT 1963)

A series of triaxial tests was run on an artificial mixture (by weight) of 80% Potters flint and 20% Peerless clay, at MIT. The samples were compacted at a water content of 17.5%, 3% dry of optimum. The dry density was 1.6 Mg/m³ (100 lb/ft³). The specimens were failed at a constant water content. The saturated specimens gave an effective angle of internal friction $\phi' = 35.6°$ and an effective cohesion $c' = 0.0$ kPa. The results are summarized in Table 3. Figure 6 shows a plot of $(\Delta\tau_d \cos\psi')$ versus $(u_a - u_w)$ and yields an angle $\alpha = 2.4°$. The corresponding angle ψ'' is 2.8° and ϕ'' is 3.4°. The ϕ^b angle is 37.8°. These results show the opposite behavior to that reported in parts (a) and (b). All samples were tested at low confining pressures. There is considerable scatter in the data (Fig. 6) and the authors are not definite as to its interpretation. The results would indicate that a decrease in pore-water pressure increases the frictional resistance of the soil more than a corresponding increase in confining pressure.

Summary

The three sets of data are considered to be analyzed in terms of two independent sets of stress variables. Two possible forms for the shear strength equation are given by [1] and [4].

The graphical form of [1] and [4] are shown in Fig. 7 using data on the compacted shale from Bishop *et al.* (1960). The authors suggest that the second form (i.e. [4]) will prove to be the most useful form in engineering practice. Further testing using other soils will improve our understanding of the shear strength of unsaturated soils.

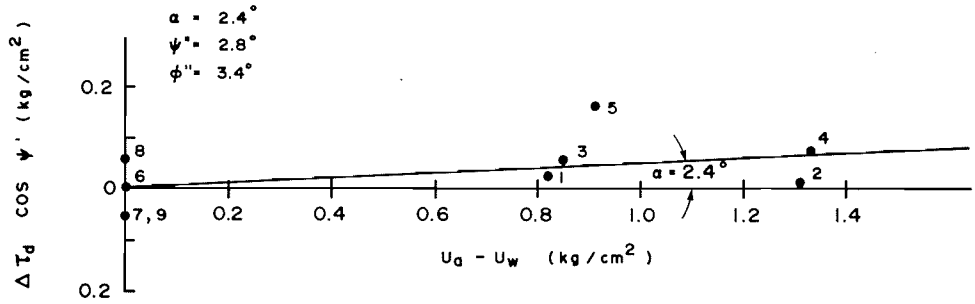

FIG. 6. Change in shear strength from saturated strength plane for Potters flint and Peerless clay.

TABLE 3. MIT results for Potters flint and Peerless clay (MIT 1963)

Test No.	Sample	$\frac{1}{2}(\sigma_1 - \sigma_3)$ (kg/cm²)	$\frac{1}{2}(\sigma' + \sigma_3')$ (kg/cm²)	$\sigma_3 - u_a$ (kg/cm²)	$u_a - u_w$ (kg/cm²)	Calculated $\frac{1}{2}(\sigma_1 + \sigma_3) - u_w$ (kg/cm²)	Calculated* $\frac{1}{2}(\sigma_1 - \sigma_3)$ (kg/cm²)	$\Delta\tau_d$ (kg/cm²)	$\Delta\tau_d \cos\psi'$ (kg/cm²)
1	SB-1	1.41		0.14	0.82	2.37	1.380	0.030	0.026
2	SB-2	2.05		0.14	1.31	3.50	2.037	0.013	0.011
3	SD-1	1.54		0.14	0.85	2.53	1.472	0.067	0.058
4	SB-4	2.26		0.14	1.33	3.73	2.171	0.089	0.077
5	SD-2	2.60		0.63	0.91	4.14	2.410	0.190	0.165
Saturated									
6	SA-1	2.325	4.000				2.320	0.005	0.004
7	SA-2	3.100	6.425				3.150	−0.050	−0.043
8	SA-3	3.950	6.700				3.890	0.060	0.052
9	SA-4	4.050	7.050				4.100	−0.050	−0.043

*The calculated value refers to the shear stress on the saturation failure envelope.

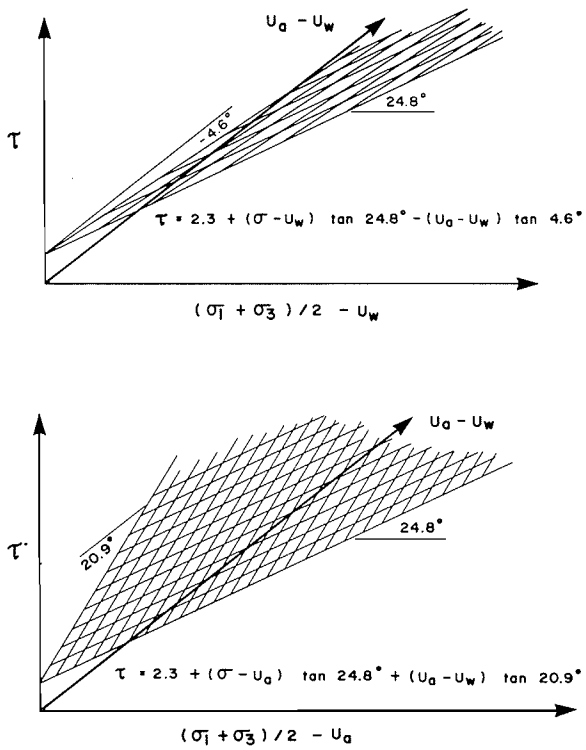

FIG. 7. Graphical form of [1] and [4] for compacted shale data.

Acknowledgements

The authors wish to acknowledge the financial support of the Department of Highways, Government of Saskatchewan, for their financial support of the research work presented in this paper.

AITCHISON, G. D. 1967. Separate roles of site investigation, quantification of soil properties, and selection of operational environment in the determination of foundation design on expansive soils. Proceedings, 3rd Asian Regional Conference on Soil Mechanics and Foundation Engineering, Vol. 2, Haifa, Israel.

BARDEN, L., MADEDOR, A. O., and SIDES, G. R. 1969. Volume change characteristics of unsaturated clay. ASCE Journal of the Soil Mechanics and Foundations Division, **95**(SM1), pp. 33–51.

BISHOP, A. W., and BLIGHT, G. E. 1963. Some aspects of effective stress in saturated and unsaturated soils. Geotechnique, **13**, pp. 177–197.

BISHOP, A. W., ALPAN, I., BLIGHT, G. E., and DONALD, I. B. 1960. Factors controlling the strength of partly saturated cohesive soils. Research Conference on Shear Strength of Cohesive Soils, ASCE, University of Colorado, Boulder, CO.

BRACKLEY, I. J. A. 1971. Partial collapse in unsaturated expansive clay. Proceedings, 5th Regional Conference on Soil Mechanics and Foundation Engineering, South Africa, pp. 23–30.

BURLAND, J. B. 1965. Some aspects of the mechanical behavior of partly saturated soils. *In* Moisture equilibrium and moisture changes in soils beneath covered areas. Butterworth and Company (Australia) Ltd., Sydney, Australia.

COLEMAN, J. D. 1962. Stress/strain relations for partly saturated soil. Correspondence. Geotechnique, **12**(4), pp. 348–350.

FREDLUND, D. G. 1974. Engineering approach to soil continua. Proceedings, 2nd Symposium on the Applications of Solid Mechanics, Hamilton, Ont., Vol. 1, pp. 46–59.

FREDLUND, D. G., and MORGENSTERN, N. R. 1976. Constitutive relations for volume change in unsaturated soils. Canadian Geotechnical Journal, **13**, pp. 261–276.

——— 1977. Stress state variables for unsaturated soils. ASCE Journal of the Geotechnical Engineering Division, 107(GT5), pp. 447–466.

MARANHA DAS NEVES, E. 1971. The influence of negative pore water pressures on the strength characteristics of compacted soils. Publication No. 386, National Laboratory of Civil Engineering, Lisbon, Portugal. (In Portuguese.)

Massachusetts Institute of Technology. 1963. Engineering behavior of partially saturated soils. Phase Report No. 1 to U.S. Army Engineers Waterways Experimental Station, Vicksburg, Mississippi. The Soil Engineering Division, Department of Civil Engineering, Massachusetts Institute of Technology, Contract No. DA-22-079-eng-288.

MATYAS, E. L., and RADHAKRISHNA, H. S. 1968. Volume change characteristics of partially saturated soils. Geotechnique, **18**(4), pp. 432–448.

SRIDHARAN, A. 1968. Some studies on the strength of partly saturated clays. Ph.D. thesis, Purdue University, Lafayette, IN.

WIDGER, R. A. 1976. Slope stability in unsaturated soils. M.Sc. thesis, University of Saskatchewan, Saskatoon, Sask.

Appendix—Stress Point Method to Obtain the Shear Strength Parameters

This appendix derives the mathematical relationship between the stress points at the top of a stress circle and the failure surface for an unsaturated soil (Widger 1976). The stress variables are $[\frac{1}{2}(\sigma_1 + \sigma_3) - u_w]$ and $(u_a - u_w)$. Figure A1 views the strength data parallel to the $(u_a - u_w)$ axis. The conversions for the zero matrix suction plane (Bishop *et al.* 1960) are

[A1] $$\sin \phi' = \tan \psi'$$

and

[A2] $$c' = d'/\cos \phi'$$

where ψ' = angle of the line through the stress point at the top of the stress circles and d' = the intercept formed by the line through the stress points.

It is also necessary to convert the angle ϕ'' for the unsaturated case. From the definition of ϕ'',

[A3] $$\tan \phi'' = \Delta\tau_c/(u_a - u_w)$$

and

[A4] $$\tan \psi'' = \Delta\tau_d/(u_a - u_w)$$

where ψ'' = angle between the line through the stress points and the $(u_a - u_w)$ axis, $\Delta\tau_c$ = change in shear strength between the saturated soil failure envelope and the failure envelope corresponding to a particular $(u_a - u_w)$ value, $\Delta\tau_d$ = change in shear strength between the saturated soil envelope through the stress points and the envelope through the stress points at a particular $(u_a - u_w)$ value.

The matrix suction is the same value in [A3] and [A4] and therefore

[A5] $$(\tan \phi'')/\Delta\tau_c = (\tan \psi'')/\Delta\tau_d$$

Considering the shear strength axis gives

[A6] $$\Delta\tau_c = c_s' - c'$$

and

[A7] $$\Delta\tau_d = d_s' - d'$$

where c_s' = the cohesion intercept of the failure envelope at a matrix suction $(u_a - u_w)$ and d_s' = the cohesion intercept at a matrix suction $(u_a - u_w)$ using the stress point method. Since ϕ' is constant for all matrix suction values,

[A8] $$\Delta\tau_d = (c_s' - c') \cos \phi'$$

Substituting [A6] and [A8] into [A5] gives

[A9] $$\tan \phi'' = \frac{\tan \psi''}{\cos \phi'}$$

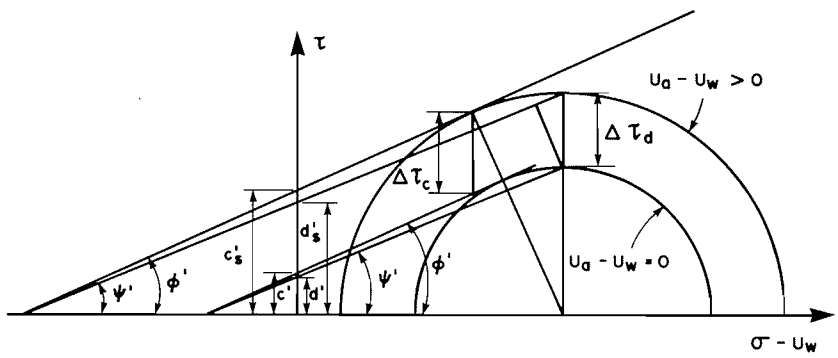

FIG. A1. Failure circles looking parallel to $(u_a - u_w)$ axis to compare failure envelopes.

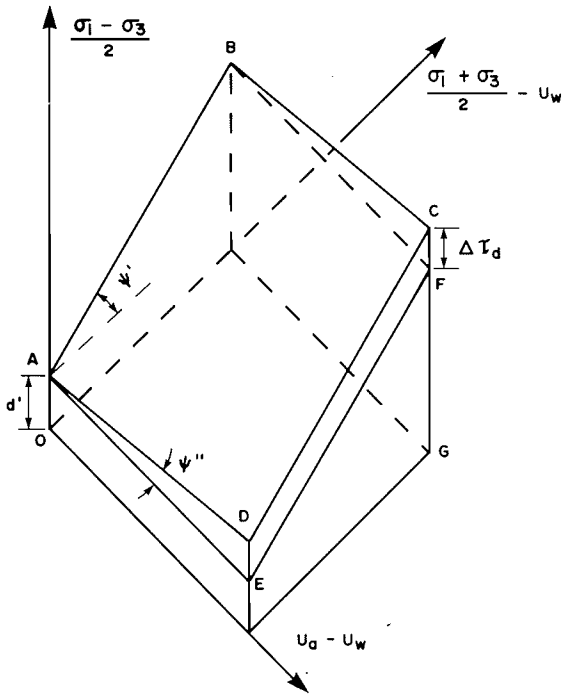

FIG. A2. Three-dimensional failure surface using the stress point method.

In order to compute ϕ'', it is necessary to obtain ψ''. The procedure that appears most convenient involves the use of the stress point method failure surface (Fig. A2). Imagine viewing along the failure envelope for a saturated soil (plane ABFE); if the matrix suction variable does not affect the shear strength, the three-dimensional failure surface as viewed along the matrix suction axis appears as a line. However, the change in shear strength ($\Delta\tau_d$) must be multiplied by cos ψ' in order to transform it into a line perpendicular to the saturation failure plane (Fig. A3). Let the slope of the plot of ($\Delta\tau_d$ cos ψ') versus matrix suction be tan α.

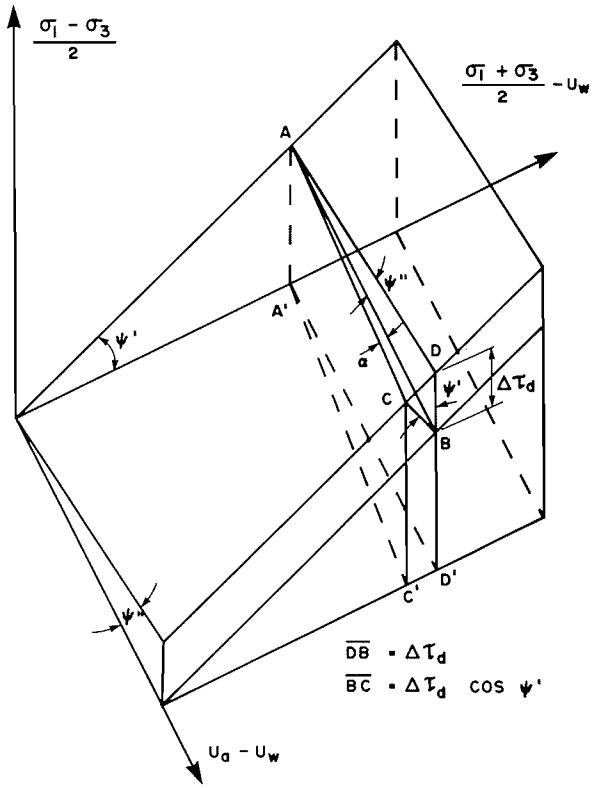

FIG. A3. Failure surface showing projection of shear strength onto the saturated strength plane.

$$[A10] \qquad \tan\alpha = \frac{\Delta\tau_d \cos\psi'}{u_a - u_w}$$

Substituting [A4] into [A10] gives

$$[A11] \qquad \tan\psi'' = \frac{\tan\alpha}{\cos\psi'}$$

The value of tan ϕ'' can now be computed from [A9].